*JOURNAL OF NANO- AND ELECTRONIC PHYSICS*
Vol. **8** No 4(1), 04025(4pp) (2016)

*ЖУРНАЛ НАНО- ТА ЕЛЕКТРОННОЇ ФІЗИКИ*
Том **8** № 4(1), 04025(4cc) (2016)

# Synthesis and Nanoscale Characterization of $LiNbO_3$ Thin Films Deposited on $Al_2O_3$ Substrate by RF Magnetron Sputtering under Electric Field

R.N. Zhukov*, D.A. Kiselev, K.D. Shcherbachev, M.I. Voronova, S.V. Ksenich, I.V. Kubasov, A.A. Temirov, N.G. Timushkin, M.V. Chichkov, A.S. Bykov, M.D. Malinkovich, Yu.N. Parkhomenko

*National University of Science and Technology "MISiS", 4, Leninskiy pr., 119049 Moscow, Russian Federation*

(Received 18 October 2016; published online 29 November 2016)

$LiNbO_3$ thin films were deposited on $Al_2O_3$ substrates by RF-magnetron sputtering with in-situ electric field to study the self-polarization effect. The films have been characterized crystallographically by x-ray diffraction, and morphologically by atomic force microscopy. The films contain crystallites of $LiNbO_3$ with preferable orientation [012] along the normal to the $Al_2O_3$ substrate surface (012). Piezoresponse force microscopy was used to study vertical and lateral polarization direction in $LiNbO_3$ thin films. The analysis of the histograms of vertical piezoresponse images allowed to reveal self-polarization effect in films. The local piezoelectric hysteresis performed on the nanometer scale indicates switching behavior of polarization for $LiNbO_3$ thin film.

**Keywords:** Lithium niobate, Rf-magnetron sputtering, Self-polarization, Piezoresponse force microscopy.

DOI: 10.21272/jnep.8(4(1)).04025 PACS numbers: 77.80.Dj, 68.55. – a, 77.55.H –

## 1. INTRODUCTION

Ferroelectric thin film integration with Si and other integrated device substrates has the potential to enable new modes of photonics integration as well as a new class of high work/volume piezoelectric devices for MEMS integration. Thin films of Lithium Niobate ($LiNbO_3$) posses a number of advantages over bulk material including the possibilities of producing step index profiles, selectively introducing dopants, and the fabrication of multilayer structures.

Less daunting is the development of a hybrid device in which the infrared source and frequency doubling waveguide are formed on different substrates, precluding the need for a cladding layer and allowing the use of a more compatible substrate for the growth of the ferroelectric thin film.

The ferroelectric thin films are intensively investigated because of their useful ferroelectric, piezoelectric, pyroelectric, and electrooptic properties and nonvolatile ferroelectric memories [1]. It is often observed that films prepared by different deposition techniques on different substrates possess a significant polarization (self-polarization) that may be almost as high as that produced by the subsequent poling [2 and references therein]. The observation of a self-polarization state in different systems is frequently associated with various factors such as thickness, texture, different substrates/electrodes and the formation temperature of the ferroelectric phase.

The self-polarization effect has been explained in terms of a space charge associated with the Schottky barriers located at the bottom film-electrode interface [2] or by a mechanical coupling between the ferroelectric film and the rigid substrate [3]. Piezoresponse force microscopy (PFM) is one of the most powerful techniques used for imaging and identifying domains in a ferroelectric and piezoelectric materials at nanoscale [4]. Recently, PFM method has be used to probe the self-polarization effect at the nanoscale level in ferroelectric materials as $Pb(Zr_xTi_{1-x})O_3$ [5-7], $Pb_{1-x}La_x(Zr_{1-y}Ti_y)_{1-x/4}O_3$ [8] and $Hf_{0.5}Zr_{0.5}O_2$ [9] thin films. In addition, it was reported that PZT and PLZT thin films with different thickness had influence on the self-polarization effect.

Only very recently Kiselev et. al. showed that the RF magnetron sputtering of a target allows the synthesis of thin (~ 100 nm) lithium-niobate films on single-crystal silicon substrates with a high (up to 65 %) degree of orientation of grains in which the polarization vector is perpendicular to the substrate plane and piezoelectric characteristics of the films greatly depend on the crystallographic orientation of the silicon substrates [10].

In this paper, we continued to study influence of the type and crystallographic orientation of the substrate on the domain structure, self-polarization effect and piezoelectric properties of the films of lithium niobate. $Al_2O_3$ plate was used as substrate whose orientation is different from the c-direction; film deposition was carried out by RF-magnetron sputtering target under the simultaneous action of electric field directed toward or away from the substrate.

## 2. EXPERIMENTAL DETAILS

The $LiNbO_3$ films 100 nm thick were deposited on $Al_2O_3$ (012) substrate by RF magnetron sputtering of the single-crystalline target in Ar/O = 1 atmosphere. The magnetron power was 150 W. To investigate influence polarity of the electric field on self-polarization, we performed the following procedure the synthesis $LiNbO_3$ films in in-situ electric filed (Fig. 1). The top side of $Al_2O_3$ substrate was coated Ta (electrode #1), second electrode (electrode #2) placed at a distance of about 15 cm from its bottom substrate. During the process of deposition between Electrode №1 and Electrode №2 was applied DC voltage: i) + 500 V and

* rom_zhuk@mail.ru

 

ii) – 500 V, thus the electric field intensity was about 33-35 V/cm.

In next we called a samples synthesized in positive electric field as "$LiNbO_3/Al_2O_3$-@plus" (positive potential on electrode #1), in negative field "$LiNbO_3/Al_2O_3$-@minus".

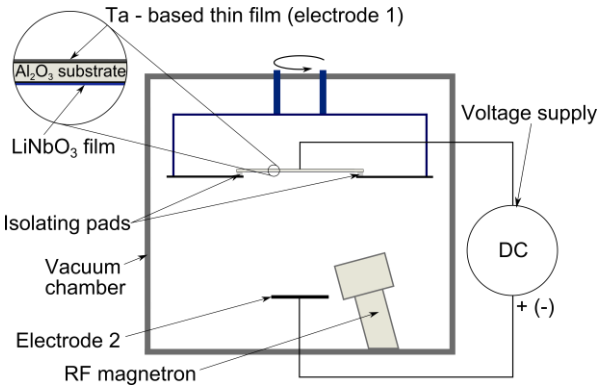


**Fig. 1** – Schematic representation deposition of lithium niobate thin film on $Al_2O_3$ substrate under in-situ electric field

The phase composition of the films was determined by X-ray diffraction on diffractometer D8 Discover (Bruker-AXS, Germany). The X-ray source used was a copper anode X-ray tube. To increase the intensity of monochromatization and collimation in the diffraction plane, we used a Göbel mirror. The width of the x-ray beam irradiated the samples was of 0.2 mm. Angular distribution of the diffracted beam was measured using Bruker LynxEye 1D detector. The measurements were performed in $2\theta$-$\omega$ geometry. Experimental data were analyzed using the EVA program (incorporated into the D8 Discover diffractometer software package) and ICDD PDF-2 database.

The surface morphology, and piezoelectric properties of the $LiNbO_3$ thin films were characterized by the piezoresponse force microscopy using commercial scanning probe microscopes MFP-3D (Asylum Research) with Asyelec Ti/Ir coated conductive probes (Asyelec-01, Asylum Research, USA). Vertical or out-of-plane PFM (OOP-PFM) and lateral/in-plane PFM (IP-PFM) images of the samples were obtained by applying AC voltage (3V peak-to-peak) with the frequency around 300 kHz.

## 3. RESULTS

XRD diffraction pattern are shown in Fig. 2. To avoid a strong reflection (012) type from the substrate, the ω start position were shifted for 2° from $2\theta/2$ value.

It was found out that the both films contain crystallines of $LiNbO_3$ with preferable orientation [012] along the normal to the $Al_2O_3$ substrate surface (012). However, in a case of @plus sample, the crystallines with planes of (110) type, which are parallel to the sample surface, are also revealed.

The surface morphology of the $LiNbO_3$ films synthesized on $Al_2O_3$ substrate with external electric field shown in Fig. 3 (a, b). On the topographic images a well visualized two types grains: i) "big" grains with the lateral grain size of which ranged from 300 to 600 nm and 40-80 nm in height and ii) "small" grain with 5 nm high and 50 nm in diameter.

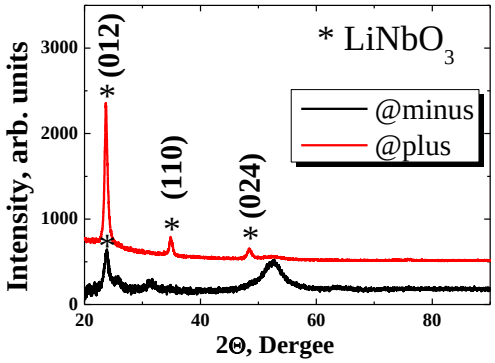


**Fig. 2** – X-ray diffraction patterns of an as-grown $LiNbO_3$ on $Al_2O_3$ substrate

From the statistical analysis of the topography the lithium niobate thin films found that its roughness ($R_{ms}$) ~23 nm for sample $LiNbO_3/Al_2O_3$ - @plus and 8 nm for $LiNbO_3/Al_2O_3$ – @minus.

OOP-PFM and IP-PFM images obtained simultaneously with the topography image are shown in Fig. 3 (c-f) for both samples. As known, PFM can to use to characterize the polarization states in the ferroelectric materials.

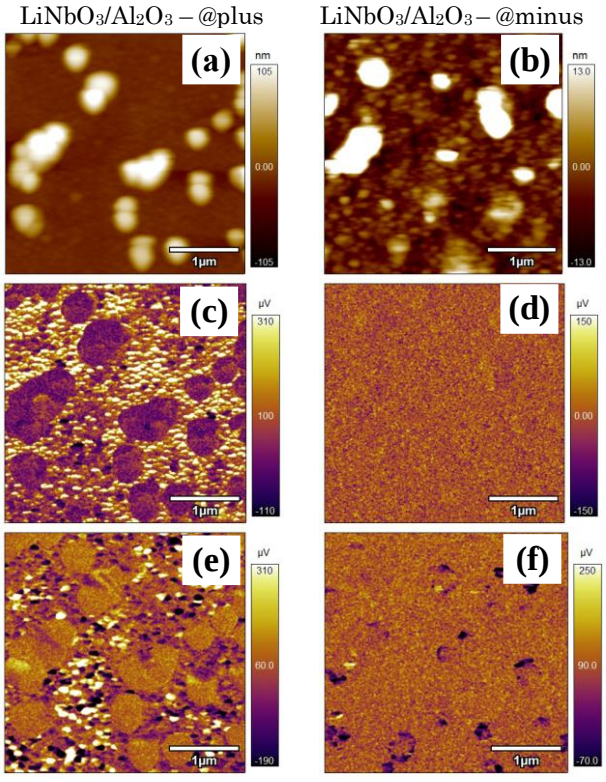


**Fig. 3** – Topography (a, b), OOP-PFM (c, d) and IP-PFM (e, f) images of $LiNbO_3/Al_2O_3$ heterostructures

In addition, the "bright" and "dark" contrasts of grains on the OOP piezoresponse signal (Fig. 3 c, d), corresponding to a particular direction of the polarization vector, there is "zero" contrast, which corresponds to the presence of the non-ferroelectric

particle, for example the secondary phase $LiNb_3O_8$, observed previously in sol-gel derived $LiNbO_3$ films [11] In our case, the maximum piezoelectric response (positive value a signal or "bright" contrast) observed in the film, which implies that the polarization vector in this area is directed toward the lower interface. In IP-PFM images (Fig. 3 e, f), we visualize the piezoresponse corresponding to the polarization direction in the plane of the film, which corresponds to the piezoelectric modulus $d_{15}$. The good lateral piezoresponse signal was observed in sample $LiNbO_3/Al_2O_3$-@plus, and these results correlate well with XRD data. Again, as an on OOP-PFM image in IP-PFM signal we not have contrast from "big" grain, that confirms non-ferroelectric nature this particles.

Fig. 4 shows the OOP-PFM histograms of $LiNbO_3$ films acquired from piezoelectric out-of-plane images in Fig. 3 (c, d) for two samples. As known, the piezohistograms are statistical distributions of the piezoelectric signal related to the domain configuration in a ferroelectric such as for out-of-plane polarization the vertical tip displacement is due to the effective $d_{33}$ piezoelectric coefficient. Thus, the observed peaks in these distribution curves are associated with the most probable domain configuration while the peak width is a measure of a number of domain states [8].

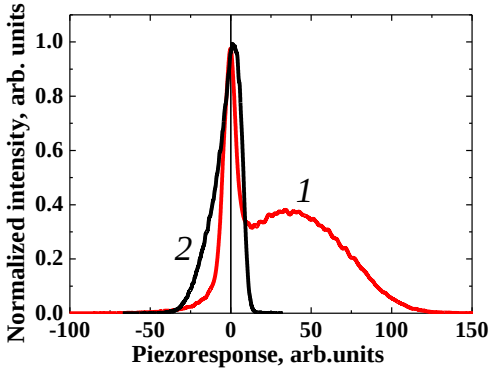


**Fig. 4** – OOP-PFM histograms distribution of $LiNbO_3/Al_2O_3$: curve 1 – $LiNbO_3/Al_2O_3$ – @plus, curve 2 – $LiNbO_3/Al_2O_3$ – @minus

As can see from Fig. 4 (curve 1), for sample $LiNbO_3/Al_2O_3$-@plus, the maximum of the OOP-PFM histogram of this distribution is shifted toward positive values of the piezoelectric response (~ 50), which implies that the polarization vector in most ferroelectric active grains is directed toward the lower interface. In contrast, for sample $LiNbO_3/Al_2O_3$-@minus the maximum slightly shifted to negative value (~ – 10). The asymmetry of the distribution of the OOP-PFM signal is a manifestation of the so-called self-polarization effect. The peaks "0" (zero piezoresponse) poses a signal from "non-ferroelectric" grains.

Finally, remnant loops have been performed on the samples. Hysteresis in PFM is fundamentally different than hysteresis in a macroscopic sample. Macroscopic hysteresis occurs due to the nucleation growth and interaction of multiple separated domains, while in PFM, nucleation of a single domain occurs under a sharp tip and PFM signal follows the development of domains at a single location. Here, the remnant piezoresponse has been measured in 30 ms after the removal of the DC pulse (duration 30 ms).

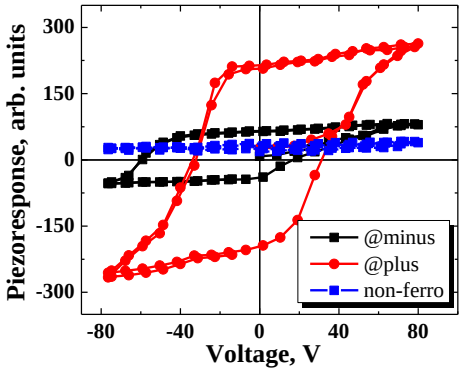


**Fig. 5** – Remnant piezoelectric hysteresis loops of the $LiNbO_3/Al_2O_3$

An example of the resulting nanoscale piezoelectric hysteresis loops was measured in ferroelectric active areas of the both $LiNbO_3$ thin films by applying cycles of 80 V at the PFM tip, as shown in Fig. 5. The range of switching voltages was determined from the local piezoresponse hysteresis loops. The loop for sample $LiNbO_3/Al_2O_3$-@plus is almost symmetrical and characterized the bigger remnant piezoelectric response (four times) compared with loop for $LiNbO_3/Al_2O_3$-@minus. On the other hand the coercive voltage for the sample $LiNbO_3/Al_2O_3$-@minus is more then sample synthesized in positive electric field. The remnant PFM signal displayed a ferroelectric character in the $LiNbO_3$ thin film. Thus, we can suppose that the local hysteresis loop is caused by local domain switching underneath the tip. In contrast, for "non-ferroelectric" grains observed no switching in OOP-PFM signal in the entire range of DC voltage.

## 4. CONCLUSIONS

In summary, $LiNbO_3$ ferroelectric films were grown on $Al_2O_3$ substrate by RF-magnetron sputtering in in-situ electrical field different polarity. The films contain crystallites of $LiNbO_3$ with preferable orientation [012] along the normal to the $Al_2O_3$ substrate surface [012] ($Al_2O_3$ and $LiNbO_3$ have trigonal crystal system). Besides together with ferroelectric phase is formed non-ferroelectric phase (as example $LiNb_3O_8$ particles). Deposition of lithium niobate films on a sapphire substrate under the action of electric field has a significant impact on their domain structure and ferroelectric properties. PFM was used to study vertical and lateral polarization direction in $LiNbO_3$ thin films. The analysis of the histograms of vertical piezoresponse images allowed to reveal self-polarization effect in films. This effect is best shown for $LiNbO_3$ film deposited in positive electric field. By this means even at low electric field intensity (~ 30 V/cm) during the synthesis observed a significant difference in OOP-PFM and IP-PFM signals for different polarity of the electric field – the presence of a large domain ordering at a positive potential on the substrate, and the almost complete lack of order at negative. Also, the local hysteresis loops are significantly different for samples grown at different

polarities of the electric field.

From the results obtained in this paper, it follows that the choice of the crystallographic direction of the substrate and the synthesis of films under the action of a electric field can have a significant impact on their domain structure and ferroelectric properties.

## ACKNOWLEDGEMENT

The studies are performed on the equipment of Center for Shared Use "Materials Science and Metallurgy" at the National University of Science and Technology "MISiS". The research was financially supported by the Federal Target Program "Investigation and Engineering in High-Priority Lines of Development of Science and Technology in Russia for 2014–2020" (unique project identifier RFMEFI57814X0071, contract no. 14.578.21.0071).

## REFERENCES

1. J.F. Scott, *Ferroelectric Memories* (2000).
2. A.L. Kholkin, K.G. Brooks, D.V. Taylor, S. Hiboux, N. Setter, *Integr. Ferroelectr.* **22**, 525 (1998).
3. A. Gruverman, B.J. Rodriguez, A.I. Kingon, *Appl. Phys. Lett.* **83**, 728 (2003).
4. A.L. Kholkin, V.V. Shvartsman, D.A. Kiselev, I.K. Bdikin, *Ferroelectrics* **341**, 3 (2006)
5. A. Wu, P.M. Vilarinho, V.V. Shvartsman, G. Suchaneck, A.L. Kholkin, *Nanotechnology* **16**(1), 2587 (2005).
6. D.A. Kiselev, A.L. Kholkin, A.A. Bogomolov, O.N. Sergeeva, E.Yu. Kaptelov, I.P. Pronin, *Tech. Phys. Lett.* **34**(8), 646 (2008).
7. E.C. Lima, E.B. Araújo, A.G Filho, A.R. Paschoal, I.K. Bdikin, A.L. Kholkin, *J. Phys. D: Appl. Phys.* **45**(21), 215304 (2012).
8. M. Melo, E.B. Araújo, V.V. Shvartsman, V.Ya. Shur, A.L. Kholkin, *J. Appl. Phys.* **120**, 054101 (2016).
9. Z. Fan, J. Xiao, J. Wang, et al., *Appl. Phys. Lett.* **108**, 232905 (2016).
10. D.A. Kiselev, R.N. Zhukov, S.V. Ksenich et al., *J. Surf. Investig. X-Ray* **10**, 742 (2016).
11. F. Johann, T. Jungk, S. Lisinski et al., *Appl. Phys. Lett.* **95**, 202901 (2009).